Preprints of the 19th World Congress
The International Federation of Automatic Control
Cape Town, South Africa. August 24-29, 2014

Sliding Mode Prediction Control for 3D Path Following of An Underactuated AUV

Li-Jun Zhang *. He-Ming Jia. Da-Peng Jiang*****

**School of Marine Engineering, Northwestern Polytechnical University, Xi'an, China (Tel: 86-29-88491079; e-mail: zhanglj7385@nwpu.edu.cn).*
***College of Mechanical and Electrical Engineering, Northeast Forestry University, Harbin, China (e-mail:jiaheming@nfu.edu.cn)*
****College of Shipbuilding Engineering, Harbin Engineering University, Harbin, China, (e-mail: jdp103@hrbeu.edu.cn)*

Abstract: Compared to the traditional 2D path following case, 3D path following is more complicated since the coupling effect between horizontal and vertical plane has to be taken into account. In this paper, a sliding mode prediction controller is presented, which drives an underactuated AUV to follow a desired 3D path under time-varying current disturbances. A sliding mode technique combined with the predictive control strategy is developed to compensate for the impact of the hydrodynamic damping coupling via the feedback correction and receding horizon optimization techniques. In addition, Different from the traditional reference orientation method for path following control, here a methodology named 3D virtual guidance orientation (VGO) is built to deal with the vehicle dynamics. The geometric characteristic of tracking curve is contained in the control design as an extra degree of freedom to drive the vehicle to track a virtual target along desired path. Hence, the proposed method can avoid saturation problem of driving devices (stern plane and rudder) of AUV. Numerical simulations illustrate the excellent path following performance of the AUV in 3D under the proposed control scheme.

Keywords: Underactuated AUV, 3D path following, sliding mode predictive control, visual guidance.

1. INTRODUCTION

Driving an AUV along a desired path accurately is one of the most important issues in many marine applications, including discovering offshore oil fields, scientific investigation of deep sea, exploitation of underwater resources, long range survey, oceanographic mapping, underwater pipelines tracking, military missions and so on, see Caccia. M[1999], Bandy.P.R[2005], Calyo. O.[2009]. In most studies for path following problems of the AUV, the assumptions for the coupling interactions between horizontal and vertical plane are ignored, see Lionel L.[2007], Li J.H.[2005] and Carlos S.[2009]. But in the 3D maneuvering case, the coupling influence on the tracking precision is distinct since the velocity and acceleration in the direction of each DOF of the AUV is coupled dramatically.

One challenge for 3D path following of an AUV is that the considered system is underactuated. In order to address the underactuated control problem, some researchers concentrate their interests on the applications of reference model method to this control problem, see Li J.H.[2005], Antonelli G.[2003]. This method are far from effective one since the complex computation of desired reference orientation, especially，the hydrodynamic model of an AUV in 3D is highly nonlinear and uncertain, so it is almost impossible to generate a desired reference trajectory by an accurate model. Another challenge is the complex nonlinearity of either dynamics or kinematics in 3D model. Many researchers make their efforts to apply nonlinear design methodologies to this problem. Encarnasiio P.[2000] studied the time-varying hydrodynamic parameters based on Lyapunov stability theorem. Antonelli G.[2006] provided an adaptive technique to investigate the 6-DOF AUV control problem using the similar scheme. Most papers published on above topic adopt the backstepping technique as the design method(see K.Do[2003], Fossen, T.I.[2002]). However, the above control approaches have to closely depend on the known nonlinear model as a prior. But a new issue arises, for example, the hydrodynamic coefficients are too much difficult to obtain since the complicated nonlinear coupling interactions between horizontal and vertical plane in the 3D motion, and the more complicated control is not suitable for the engineering application.

Motivated by the above discussion, this paper presents a virtual guidance orientation (VGO) technique under a Serret-Frenet(SF) coordinate frame to investigate the path following problem of the AUV. The idea of VGO appeared for the first time in the work of Micaelli A.et al. [1993]. Immediately, Del. Rio.et al. [2002] explored the concept of a virtual target for the path following of wheeled robots. A recent publication extended the idea exploited in Micaelli A.et al. [1993] to the control scheme of marine vehicle in Lionel L.[2007]. Compared with the traditional method (way-point tracking), the advantage of VGO method is that it intuitively explains the physical and geometric essence of the tracking motion of the vehicle, and also avoids the saturation problem of driving devices (stern plane and rudder) of the AUV.

To improve the performance of tracking controller of the AUV, a composite control scheme, called sliding mode prediction control (SMPC), combined with sliding mode control (SMC) and linear predictive control (LPC) technique is applied in this paper. The SMPC strategy have the following advantages: 1) it can overcome the chattering of the SMC while improving the robustness of the SMC with the help of the LPC; 2) the boundaries of uncertainties may be unknown, so the conservation is decreased; 3) feedback correction and receding horizon optimization in the LPC are applied to compensate the influence of uncertainties in time, and the control signal can be optimized continual and online. More specifically, a sliding mode prediction controller is proposed in which the predictive information of sliding mode is used. By constructing the predictive value of sliding mode which tracks the desired sliding mode reference value, the reaching ability of sliding mode is achieved. And then through the feedback correction and receding horizon optimization, a 3D path following controller is obtained which guarantees the tracking error is robustly stable and all the state signals are bounded. Finally, the tracking performances are studied through numerical simulations.

2. PROBLEM FORMULATION

2.1 Path Tracking Error System of AUV Based on VGO

This subsection first introduces the modelling of the AUV in 3D space, then extends the concept of the VGO from 2D space to 3D space. Based on the idea of VGO in 3D space, a 3D path following error system is fully constructed. A diagram of spatial path following of the AUV is shown as Fig. 1, where {I}, {F} and {B} are represented as an earth-fixed frame, a S-F frame and a body-fixed frame, respectively. Denote by $U_B=\sqrt{u^2+v^2+w^2}$ a total speed of the vehicle; denote by $path$ a desired spatial tracking path.

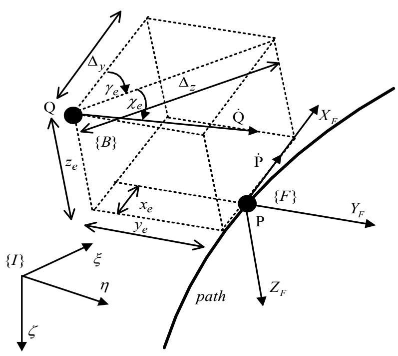

Fig. 1. diagram of VGO-based path following in 3D.

Assume that Q is the real mass point of the AUV. In frame $\{I\}$, the inertial position and velocity vectors are denoted by $\mathrm{Q}=[\xi,\eta,\zeta]^{\mathrm{T}}$ and $\dot{\mathrm{Q}}=[\dot{\xi},\dot{\eta},\dot{\zeta}]^{\mathrm{T}}$, respectively; then $U=\|\dot{\mathrm{Q}}\|=\sqrt{\dot{\mathrm{Q}}^{\mathrm{T}}\dot{\mathrm{Q}}}$ denotes the magnitude of the total velocity; the azimuth angle of the AUV $\gamma_Q=\arctan(\dot{\eta}/\dot{\xi})$;the angle of pitch $\chi_Q=\arctan(\dot{\zeta}/\sqrt{\dot{\xi}^2+\dot{\eta}^2})$ .In the course of movement of the AUV, there are always the stacking angle α and the drift angle β, so the actual yaw angle ϕ and pitch angle θ of the vehicle are:

$$\begin{aligned}\phi&=\gamma_Q-\beta\\ \theta&=\chi_Q-\alpha,\end{aligned}\tag{1}$$

then the kinematics equation of the AUV can be represented as in frame $\{I\}$:

$$\begin{cases}\dot{\xi}=U_B\cos\gamma_Q\cos\chi_Q\\ \dot{\eta}=U_B\sin\gamma_Q\cos\chi_Q\\ \dot{\zeta}=U_B\sin\chi_Q\\ \dot{\chi}_Q=q+\dot{\alpha}\\ \dot{\gamma}_Q=r/\cos\theta+\dot{\beta}\end{cases}\tag{2}$$

where r is the vehicle's angular speed (yaw rate). Now rotate the coordinate frame $\{B\}$ to the flow frame $\{W\}$, denote by $(Q;x_W,y_W,z_W)$, such that the direction of the total velocity U_B is aligned with x_W axis. Let $W_{RB}(\gamma_Q,\chi_Q)$ denote the rotation matrix from $\{B\}$ to $\{W\}$. Clearly, in the flow frame $\{W\}$, the linear velocity vector is expressed as $W_{VB}=(U_B,0,0)^T$. Assume the desired $path$ is a parameter continuous smooth curve with any given point p be the "virtual vehicle" which moves along the $path$ at a desired speed. Now construct a S-F frame $\{F\}$ with the point p be its coordinate origin. The moving coordinate frame $\{F\}$ is denoted by $(p;x_F,y_F,z_F)$ (see Fig. 1.), where unity vectors x_F is the tangent vector, y_F is the principal normal vector, z_F is the binormal vector, and $z_F=x_F\times y_F$. The curvature and torsion of the $path$ are denoted by $c_1(\mu)$ and $c_2(\mu)$ respectively, which are continuous and bounded, where μ denotes the arc length of the $path$. According to the well-known S-F frame, the angular velocity, denote by $SF_{\omega SF}(\gamma_Q,\chi_Q)$, of the "virtual target" p in frame $\{I\}$ can be expressed in $\{F\}$ to yield

$$SF_{\omega SF}(\gamma_Q,\chi_Q)=(0,c_2(\mu)\dot{\mu},c_1(\mu)\dot{\mu})^T\tag{3}$$

Correspondingly, the velocity vector of point p in frame $\{I\}$ can be expressed as $SF_{VSF}=(U_p,0,0)^T$ in the frame $\{F\}$, where U_p is the linear vector of point p.

Next we begin to formulate the error tracking systems. Let x_e,y_e,z_e denote the signed distances between the vehicle center of mass and the origin of the S-F frame along the coordinate axes x_F,y_F,z_F, say $SF_{PorgW}=(x_e,y_e,z_e)^T$. In other words, SF_{PorgW} represents the coordinate of point Q in frame $\{F\}$. With this notation, the relative velocity between $\{W\}$ and $\{F\}$ can expressed as

$$\frac{dSF_{PorgW}}{dt} = (\dot{x}_e, \dot{y}_e, \dot{z}_e)^T .$$

Let $SF_{RW}(\phi_e, \theta_e)$ be rotation matrix between $\{F\}$ and $\{W\}$, it follows (see Greiner W. [2004])

$$SF_{RW}(\phi_e, \theta_e) W_{VB} = SF_{VSF} + \frac{dSF_{PorgW}}{dt} + SF_{\omega SF} \times SF_{PorgW} \tag{4}$$

where

$$SF_{\mathrm{RW}} = \begin{bmatrix} \cos\phi_{\mathrm{e}}\cos\theta_{\mathrm{e}} & -\sin\phi_{\mathrm{e}} & \cos\phi_{\mathrm{e}}\sin\theta_{\mathrm{e}} \\ \sin\phi_{\mathrm{e}}\cos\theta_{\mathrm{e}} & \cos\phi_{\mathrm{e}} & \sin\phi_{\mathrm{e}}\sin\theta_{\mathrm{e}} \\ -\sin\theta_{\mathrm{e}} & 0 & \cos\theta_{\mathrm{e}} \end{bmatrix}$$

Note ϕ_e and θ_e are the yaw angle error and the pitch angle error between $\{F\}$ and $\{W\}$. From system (2) and the angular velocity (3) in the frame $\{F\}$, it follows

$$\begin{cases} \dot{\phi}_e = r / \cos\theta + \dot{\beta} - c_1(\mu)\dot{\mu} \\ \dot{\theta}_e = q + \dot{\alpha} - c_2(\mu)\dot{\mu} \end{cases} \tag{5}$$

Let $U_B = U_d$, where U_d is a desired cruise speed of the vehicle, then by Eq. (4), the kinematics error model can be expressed as follows:

$$\begin{cases} \dot{x}_e = y_e c_1(\mu)\dot{\mu} - z_e c_2(\mu)\dot{\mu} + \\ \qquad U_d \cos\phi_e \cos\theta_e - U_p \\ \dot{y}_e = -x_e c_1(\mu)\dot{\mu} + U_d \sin\phi_e \cos\theta_e \\ \dot{z}_e = x_e c_2(\mu)\dot{\mu} - U_d \sin\theta_e \\ \dot{\phi}_e = r / \cos\theta + \dot{\beta} - c_1(\mu)\dot{\mu} \\ \dot{\theta}_e = q + \dot{\alpha} - c_2(\mu)\dot{\mu} \end{cases} \tag{6}$$

System (6) is just the error tracking system. For system (6), control objective is to design variables r, q and variables U_p, μ such that the state variables x_e, y_e, z_e ϕ_e and θ_e of system (6) converge to zero.

Note that we adopt the idea of VGO, so U_p, μ can also be used to design the controller of whole system. By Lyapunov theorem, the speed of the "virtual target" U_p can be designed as

$$U_p = U_d \cos\phi_e \cos\theta_e + \kappa x_e \tag{7}$$

where $\kappa > 0$ is an adjustable gain parameter.

By the theory of classical mechanics, it is easy to get (see Greiner W.[2004])

$$\dot{\mu} = \frac{U_d \cos\phi_e \cos\theta_e + \kappa x_e}{\sqrt{x_p'^2 + y_p'^2 + z_p'^2}} \tag{8}$$

where x_p, y_p, z_p are the location of the virtual target in frame $\{I\}$, and $\phi_e = \arctan(-y_e / \Delta y)$, $\theta_e = \arctan(z_e / \Delta z)$, then Eq.(7) can be rewritten as

$$U_p = U_d \frac{\Delta_y}{\sqrt{{y_e}^2 + {\Delta_y}^2}} \frac{\Delta_z}{\sqrt{{z_e}^2 + {\Delta_z}^2}} + \kappa x_e , \tag{9}$$

where Δ_y are Δ_z are the time-varying variables. Eq. (8) and (9) will be used in the simulation study of the AUV.

2.2 Discretization of the System

Define zero-order holder for error dynamic system (6) of the AUV:

$$\dot{\lambda}(t) = \frac{\lambda(T(k+1)) - \lambda(Tk)}{T}, \tag{10}$$

Let $T = 1$, system (6) can be rewritten as:

$$\begin{cases} x_e(k+1) = c_1(\mu(k))(\mu(k+1) - \\ \qquad \mu(k)) y_e(k) - c_2(\mu(k))(\mu(k+1) - \\ \qquad \mu(k)) z_e(k) + x_e(k) + \\ \qquad U_d \cos\phi_e(k)\cos\theta_e(k) - U_p(k) \\ y_e(k+1) = -c_1(\mu(k))(\mu(k+1) - \mu(k)) x_e(k) + \\ \qquad y_e(k) + U_d \sin\phi_e(k)\cos\theta_e(k) \\ z_e(k+1) = c_2(\mu(k))(\mu(k+1) - \mu(k)) x_e(k) + \\ \qquad z_e(k) + U_d \sin\theta_e(k) \\ \theta_e(k+1) = q(k) + \alpha(k+1) - \alpha(k) - c_2(\mu(k)) \\ \qquad (\mu(k+1) - \mu(k)) \\ \phi_e(k+1) = r(k) / \cos\theta(k) + \beta(k+1) - \beta(k) - \\ \qquad c_1(\mu(k))(\mu(k+1) - \mu(k)) \end{cases} \tag{11}$$

In order to design the discrete sliding mode predictive controller, the discrete dynamic model of the AUV should be presented. Here we adopt the dynamic model as (12).

$$\begin{cases} u(k+1) = m_{vr} v(k) r(k) + m_{wq} w(k) q(k) + \\ \qquad (d_u(k) + X_{\mathrm{prop}}(k) + \omega_1(k)) / m_{11} + \\ \qquad u(k) \\ v(k+1) = (d_v(k) + \omega_2(k)) / m_{22} + v(k) + \\ \qquad m_{ur} u(k) r(k) \\ w(k+1) = (d_w(k) + \omega_3(k)) / m_{33} + w(k) + \\ \qquad m_{uq} u(k) q(k) \\ q(k+1) = (d_q(k) + M_{\mathrm{prop}}(k) + \omega_4(k)) / m_{44} + \\ \qquad q(k) \\ r(k+1) = (d_r(k) + N_{\mathrm{prop}}(k) + \omega_5(k)) / m_{55} + \\ \qquad r(k) \end{cases} \tag{12}$$

Up to now, both (11) and (12) have completely formulated the kinematics and dynamics behaviours with a set of discrete nonlinear difference equations. Next we will investigate the control design of systems (11) and (12). Define

$$\begin{aligned} x_{2i}(k) &= \left[x_e(k), y_e(k), z_e(k), \theta_e(k), \phi_e(k)\right]^{\mathrm{T}}, \\ x_{2i}(k+1) &= [x_e(k+1), y_e(k+1), z_e(k+1), \\ &\qquad \theta_e(k+1), \phi_e(k+1)]^T, i = 1 \cdots 5. \end{aligned} \tag{13}$$

Combining equation (11), (12)and (13), we have

$$\begin{cases} x_{2i-1}(k+1) = x_{2i}(k) \qquad i = 1, 2, \cdots, 5 \\ x_{2i}(k+1) = f_i(\mathbf{x}(k)) + g_i(\mathbf{x}(k))\tau_i(k) + \varpi_i(k) \end{cases} \tag{14}$$

where $f_i(X(k)), g_i(X(k))$ are given in APPENDIX.

Let $\boldsymbol{\tau}(k)=[\tau_1(k),\cdots,\tau_5(k)]=[X_{prop}(k),X_{prop}(k),$
$X_{prop}(k),M_{prop}(k),N_{prop}(k)]$

and $\varpi_i(k)$ denote the unknown terms of the system and environmental current disturbances. The control objective is to design a control law $\tau(k)$ via a sliding mode prediction control strategy, so that tracking error vector $x_{2i}(k)$ of the system asymptotically stabilize to zero while all the other state signals in the AUV control system are bounded.

3. DESIGN OF SLIDING MODE PREDICTIVE CONTROLLER

In this section, we propose a robust control law for the system (14) which is composed of sliding mode control and predictive control scheme.

3.1 The design of sliding mode prediction model(SMPM)

For system (14), defining the equalities as

$$s_i(k)=x_{2i}(k)+\sigma_i x_{2i-1}(k),\quad i=1,2,\cdots,5 \tag{15}$$

If there are σ_i such that the dynamics of system (14) is stable in the following state space

$$S=\{x(k)\,|\,s_i(x(k))=0,\quad i=1,2,\cdots,5\}, \tag{16}$$

(16) is called the sliding mode, where σ_i can be designable. In fact, based on the linear form of (15), σ_i should be chosen such that the root of $z+\sigma_i=0$ is in a right-half open unit dis. Namely, $-1<\sigma_i<0$.

In order to use predictive control strategy to improve the performance of SMC, a suitable sliding mode prediction model should be constructed at first. From Xiao L.[2007], Kim J.[2000], the following sliding mode prediction model (SMPM) is constructed:

$$s_{\mathrm{m}i}(k+1)=f_i(\mathbf{x}(k))+g_i(\mathbf{x}(k))\tau_i(k)+\sigma_i x_{2i}(k)+\gamma_i s_i(k),\quad i=1,2,\cdots,5 \tag{17}$$

where $0<\gamma_i\le 1$ are designable parameters.

3.2 The design of control

In the actual navigation of the AUV, due to time-variance, non-linearity or environmental disturbances, the proposed SMPM (17) will never completely identify the real case, so modeling errors inevitably exist. A desirable way to solve such a problem is feedback correction. The dynamics equation of the feedback correction is described as

$$\tilde{s}_{\mathrm{m}i}(k+1)=s_{\mathrm{m}i}(k+1)+\rho_i(s_i(k)-s_{\mathrm{m}i}(k)) \tag{18}$$

where $\tilde{s}_{\mathrm{m}i}(k+1)$ are the updated prediction values of sliding mode $S_{\mathrm{m}i}(k+1)$, $\rho_i\in\mathbf{R}$ are weighted feedback gains. The suitable ρ_i are chosen, the feedback correction can effectively improve the control performance. Generally, ρ_i satisfy $0<\rho_i\le 1$. For clarification, an auxiliary variable $\overline{s}_i(k)=s_i(k)-s_{\mathrm{m}i}(k)$ is used, Eq. (18) can be reduced as

$$\tilde{s}_{\mathrm{m}i}(k+1)=s_{\mathrm{m}i}(k+1)+\rho_i\overline{s}_i(k) \tag{19}$$

Since the state $\mathbf{x}_i(k)$ are measurable, $s_i(k)$ can also be obtained. Eq.(15) is rewritten as

$$s_{\mathrm{m}i}(k)=f_i(\mathbf{x}(k-1))+g_i(\mathbf{x}(k-1))\tau_i(k-1)+\sigma_i x_{2i}(k-1)+\gamma_i s_i(k-1) \tag{20}$$

Substituting Eq. (20) into Eq.(19) yields

$$\begin{aligned}\tilde{s}_{\mathrm{m}i}(k+1)&=f_i(\mathbf{x}(k))+g_i(\mathbf{x}(k))\tau_i(k)+\sigma_i x_{2i}(k)+\gamma_i s_i(k)+\rho_i\overline{s}_i(k)\\&=h_i(k)+g_i(\mathbf{x}(k))\tau_i(k)\end{aligned} \tag{21}$$

where $h_i(k)=f_i(\mathbf{x}(k))+\sigma_i x_{2i}(k)+\gamma_i s_i(k)+\rho_i\overline{s}_i(k)$.

Now, the cost function is taken as

$$\min J_i=(\tilde{s}_{\mathrm{m}i}(k+1)-s_r)^2+\lambda_i(\tau_i(k))^2,\quad i=1,2,\cdots,5 \tag{22}$$

where s_r is the sliding mode reference value. Since the control objective is to keep states on the sliding surface, so $s_r=0$. Then (20) is reduced as

$$\min J_i=(\tilde{s}_{\mathrm{m}i}(k+1))^2+\lambda_i(\tau_i(k))^2,\ i=1,\cdots,5 \tag{23}$$

where λ_i are weight coefficients. Further, according to equation (21), (23) can be rewritten as

$$\min J_i=(h_i(k)+g_i(\mathbf{x}(k))\tau_i(k))^2+\lambda_i(\tau_i(k))^2,\quad i=1,2,\cdots,5 \tag{24}$$

Then, setting the partial derivative of J_i to zero, namely $\dfrac{\partial J_i}{\partial \tau_i(k)}=0$, the optimal solution $\tau_i(k)$:

$$\tau_i(k)=-\frac{h_i(k)g_i(\mathbf{x}(k))}{g_i^2(\mathbf{x}(k))+\lambda_i},\qquad i=1,2,\cdots,5 \tag{25}$$

Further, the control inputs $X_{prop}(k),M_{prop}(k),N_{prop}(k)$ of systems (11) and (12) are also obtained.

4. ROBUST STABILITY ANALYSES

Consider system (14) and sliding mode function (15), it follows

$$\begin{aligned}s_i(k+1)&=x_{2i}(k+1)+\sigma_i x_{2i-1}(k+1)\\&=f_i(\mathbf{x}(k))+g_i(\mathbf{x}(k))\tau_i(k)+\varpi_i(k)+\sigma_i x_{2i}(k)\end{aligned} \tag{26}$$

From (23), one sees $\tau_i(k)$ affects J_i less with the decreasing of λ_i. i.e. the smaller λ_i is, the greater control signal is required to obtain optimal J_i. For simplification, according to optimal control theory, see D.J. Wang[2001], it is sound to suppose $\lambda_i(k)=0$, under the control law (25) to yield

$$\begin{aligned}s_i(k+1)&=f_i(\mathbf{x}(k))-\frac{h_i(k)g_i^2(\mathbf{x}(k))}{g_i^2(\mathbf{x}(k))+\lambda_i}+\varpi_i(k)+\sigma_i x_{2i}(k)\\&=f_i(\mathbf{x}(k))-h_i(k)+\sigma_i x_{2i}(k)+\varpi_i(k)+\frac{\lambda_i h_i(k)}{g_i^2(\mathbf{x}(k))+\lambda_i}\\&=-\gamma_i s_i(k)-\rho_i\overline{s}_i(k)+\varpi_i(k)+\frac{\lambda_i h_i(k)}{g_i^2(\mathbf{x}(k))+\lambda_i}\end{aligned} \tag{27}$$

And Eq. (20) can be described as another form

$$\begin{aligned}s_{\mathrm{m}i}(k)&=f_i(\mathbf{x}(k-1))+g_i(\mathbf{x}(k-1))\tau_i(k-1)+\sigma_i x_{2i}(k-1)+\gamma_i s_i(k-1)\\&=x_{2i}(k)-\varpi_i(k-1)+\sigma_i x_{2i-1}(k)+\gamma_i s_i(k-1)\\&=s_i(k)+\gamma_i s_i(k-1)-\varpi_i(k-1)\end{aligned} \tag{28}$$

Therefore

$$\begin{aligned}\bar{s}_i(k) &= s_i(k) - (s_i(k) + \gamma_i s_i(k-1) - \varpi_i(k-1)) \\ &= -\gamma_i s_i(k-1) + \varpi_i(k-1)\end{aligned} \tag{29}$$

Applying (29) into (27) to yield

$$\begin{aligned}s_i(k+1) &= -\gamma_i s_i(k) - \rho_i(-\gamma_i s_i(k-1) + \varpi_i(k-1)) + \varpi_i(k) + Q_{3i} \\ &= \gamma_i(-s_i(k) + \rho_i s_i(k-1)) + (\varpi_i(k) - \rho_i \varpi_i(k-1)) + Q_{3i} \\ &= Q_{1i} + Q_{2i} + Q_{3i}\end{aligned} \tag{30}$$

where, $Q_{1i} = \gamma_i(-s_i(k) + \rho_i s_i(k-1))$,

$$Q_{2i} = \varpi_i(k) - \rho_i \varpi_i(k-1), \ Q_{3i} = \frac{\lambda_i h_i(k)}{g_i^2(\mathbf{x}(k)) + \lambda_i}.$$

Theorem 1. If the change rate of disturbance is bounded, i.e., the following inequalities hold,

$$|Q_{2i}| = |\varpi_i(k) - \rho_i \varpi_i(k-1)| \le \varepsilon_i \quad i = 1, 2, \cdots, 5 \tag{31}$$

where ε_i are positive constants, then the closed-loop control system which is constructed by (11), (12) and (25), is robustly stable.

The proof is omitted, the detail is referred to Xiao L.[2000].

5. SIMULATION ANALYSES

The simulation for AUV is performed based on the semi-physical simulation platform. The desired path is considered as sine curve and the step curve. For sine curve (unit: m):

$$\begin{cases} y_P = 100\sin(\frac{x_P}{200}\pi) \\ z_P = 35 + 30\sin(\frac{x_P}{200}\pi) \end{cases} \tag{32}$$

The environmental current disturbances are (unit: kn):

$$u_{cur} = \begin{cases} 2.0 & 0\text{m} \le z \le 15\text{m} \\ 1.5 & 15\text{m} < z \le 55\text{m} \\ 1.0 & 55\text{m} < z \le 65\text{m} \end{cases} \tag{33}$$

The direction of flow is 0°. Set the initial position of the vehicle is $(x, y, z) = (0, 0, 35)(\text{m})$, initial attitude angle: $(\varphi, \theta, \phi) = (0^\circ, 0^\circ, 0^\circ)$ initial velocity: $(u, v, w) = (0, 0, 0)$, desired velocity: $u_d = 4(\text{kn})$. Considering the length characteristics of AUV and the desired curve characteristics, the gain parameter of visual guidance can be set as $\kappa = 0.05$, initial position is $(x_P, y_P, z_P) = (10, 15, 40)(\text{m})$. Choosing the control gain parameters as:

$$\begin{cases} \sigma_1 = -0.35, \sigma_2 = -0.1, \sigma_2 = -0.15 \\ \gamma_1 = \gamma_2 = \gamma_3 = 0.08 \\ \rho_1 = \rho_2 = \rho_3 = 0.9 \\ \lambda_1 = 0.15, \lambda_2 = 0.2, \lambda_3 = 0.25 \end{cases} \tag{34}$$

For step tracking curve:

$WP_1 = (80, 0, 0), WP_2 = (120, 100, 20), WP_3 = (0, 180, 40)$, initial position: $(x, y, z) = (90, -10, 0)$, initial angle: $(\psi, \theta, \phi) = (\pi/2, 0, 0)$, initial velocity: $(u, v, w) = (0, 0, 0)$, initial angular velocity: $(p, q, r) = (0, 0, 0)$, desired surge velocity: $u_d = 2(m/s)$; the controller gain can be chosen as

$$\begin{cases} \sigma_1 = -0.5, \sigma_2 = -0.2, \sigma_3 = -0.15 \\ \gamma_1 = \gamma_2 = \gamma_3 = 0.1 \\ \rho_1 = \rho_2 = \rho_3 = 0.6 \\ \lambda_1 = -0.2, \lambda_2 = -0.4, \lambda_3 = -0.5 \end{cases} \tag{35}$$

In order to verify the performance of DSMPC controller and the effectiveness of visual guidance for the spatial curve following, traditional sliding mode controller is designed to compare with DSMPC.

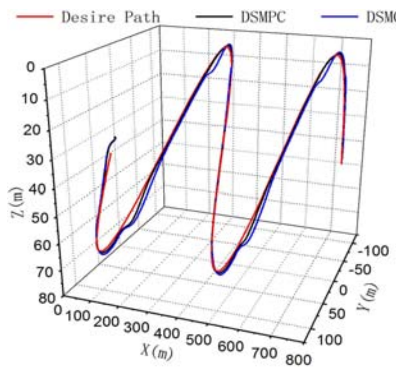

Fig. 2. AUV sine curve path following

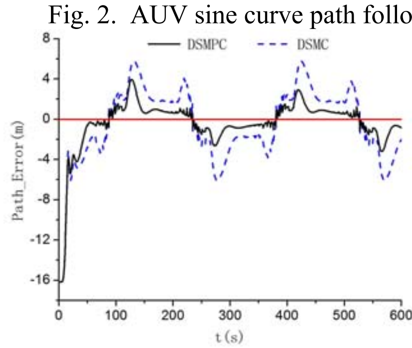

Fig. 3. Sine curve path following error

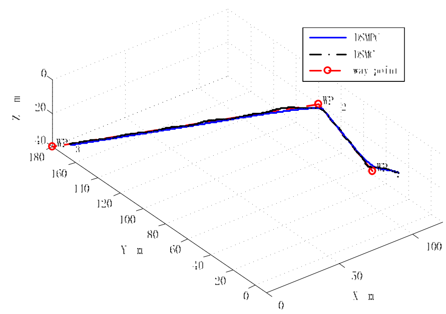

Fig. 4. 3D step path following

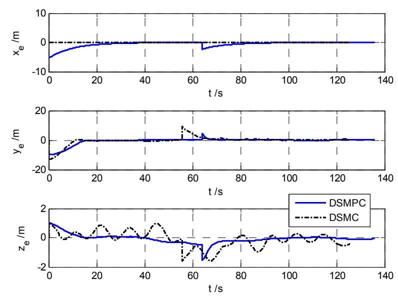

Fig. 5. 3D step curve tracking error

Fig. 2 and Fig. 3. show the tracking sine curve effects of two controllers DSMPC and DSMC. Compared with the DSMC controller, the tracking error of DSMPC controller is significantly improved. Especially, DSMPC controller can more effectively ensure the stability of system and robustness in the change of ocean current size. Fig.4. and Fig.5.show 3D step path following simulation curves. Compared with the DSMPC control method, DSMC cannot achieve fast tracking of 3D track points, and the controller based on DSMPC design is robust, even improves the accuracy of AUV 3D tracking, reduces the redundant path, there is a smaller tracking error only in path inflection point within the reasonable range.

6. CONCLUSIONS

A new sliding mode control algorithm for 3D Path following control of an underactuated AUV is presented. A sliding mode predictive control law is designed. Robust stability analysis proves that the closed-loop system has strong robustness to time-varying current disturbances with unknown boundaries. Simulation results verify the efficiency of the proposed algorithm.

REFERENCES

Caccia. M, Bono. R and Bruzzone G. B.(1999). Variable-configuration UUVs for marine science applications. *IEEE Robotics and Automation Magazine*, vol. 6, pp. 22-23.

Bandyopadhyay. P. R.(2005). Trends in biorobotic autonomous undersea vehicles. *IEEE Journal of Oceanic Engineering*, vol. 30, pp. 109-139.

Calyo. O. Sousa. A, Rozenfeld. A and Acosta G.(2009). Smooth path planning for autonomous pipeline inspections. *The 6th International Multi-Conference on Systems, Signals and Devices*, Tunisia, pp. 1-9.

Lionel Lapierre and Didik Soetanto(2007). Nonlinear path-following control of an AUV. *Ocean Engineering*, vol. 34, pp. 1734–1744.

Ji Hong Li and Pan Mook Lee(2005). A neural network adaptive controller design for free-pitch-angle diving behavior of an autonomous underwater vehicle. *Robotics and Autonomous Systems*, vol. 52(2-3), pp. 132-147.

Carlos Silvestre, Rita Cunha, Nuno Paulino, and António Pascoal(2009). A bottom-following preview controller for autonomous underwater vehicles. *IEEE Transactions on control systems technology*, vol. 17, no. 2, pp. 257-266.

Antonelli Gianluca(2003). A novel adaptive control law for underwater vehicles. *IEEE Transactions on control systems technology*, vol. 11, no. 2, pp. 221-232.

Antonelli Gianluca(2006). Adaptive/Integral actions for 6-DOF control of AUVs. *Proceedings 2006 IEEE International Conference on Robotics and Automation.* Orlando, Florida, USA, pp. 3214-3219.

P. Encarnasiio, A. Pascoal(2000). 3D Path Following for Autonomous Underwater Vehicle. *Proceedings of the 39th IEEE conference on Decision and Control.* Sydney, Australia, pp:2977-2982.

K.Do, J.Pan(2003). Robust and Adaptive path following for underacutated autonomous underwater vehicles. *Proceedings of the American Control Conference*. Denver, Colorado, pp:1994-1999.

Fossen, T. I. (2002). Marine Control Systems. Marine Cybernetics. Trondheim, Norway.

Greiner W. Classical Mechanics(2004). Point Particles and Relativity. *Springer,*New York: 72-86.

XIAO L, SU H, ZHANG X. et al. (2006). Variable structure control with sliding mode prediction for discrete-time nonlinear systems. *Journal of Control Theory and Applications*, 4(2): 140–146.

J. Kim. S.H. Oh. D. Cho and J.K. Hedrick(2000). Robust discrete-time variable structure control methods. *ASME J. Dyn. Sysl. Mea.s. Control*, pp: 766-775.

Micaelli, A., Samson, C.(1993). Trajectory tracking for unicycle-type and two-steering wheels mobile robots. *Technical Report,* No. 2097, INRIA, Sophia-Antipolis, France.

Del. Rio. F et al(2002). A new method for tracking memorized paths：applications to unicycle robots. *Proc. MED2002*, Lisbon, Portugal.

APPENDIX

$$g_1(\mathbf{x}(k)) = \frac{\cos x_9(k+1)\cos x_7(k+1)}{m_{11}\cos\alpha(k+1)\cos\beta(k+1)}$$

$$g_2(\mathbf{x}(k)) = \frac{\sin x_9(k+1)\cos x_7(k+1)}{m_{11}\cos\alpha(k+1)\cos\beta(k+1)}$$

$$g_3(\mathbf{x}(k)) = \frac{\sin x_7(k+1)}{m_{11}\cos\alpha(k+1)\cos\beta(k+1)}$$

$$g_4(\mathbf{x}(k)) = \frac{1}{m_{44}}, \quad g_5(\mathbf{x}(k)) = \frac{1}{m_{55}\cos\theta(k)}$$

$$\begin{aligned}
f_1(\mathbf{x}(k)) = {} & c_1(\mu(k+1))c_3(\mu(k+1))(\mu(k+2)-\mu(k+1))x_3(k+1)- \\
& c_2(\mu(k+1))(\mu(k+2)-\mu(k))x_5(k+1)+x_1(k+1)-U_P(k+1)+ \\
& (m_{vr}v(k)r(k)+m_{wq}w(k)q(k)+d_u(k))/m_{11}+ \\
& u(k))\cos x_7(k+1)\cos x_9(k+1)/(\cos\alpha(k+1)\cos\beta(k+1))
\end{aligned}$$

$$\begin{aligned}
f_2(\mathbf{x}(k)) = {} & -c_1(\mu(k+1))c_3(\mu(k+1))(\mu(k+2)-\mu(k))x_1(k+1)- \\
& c_1(\mu(k+1))c_4(\mu(k+1))(\mu(k+2)-\mu(k))x_5(k+1)+x_3(k+1)+ \\
& (m_{vr}v(k)r(k)+m_{wq}w(k)q(k)+d_u(k))/m_{11}+ \\
& u(k))\sin x_9(k+1)\cos x_7(k+1)/(\cos\alpha(k+1)\cos\beta(k+1))
\end{aligned}$$

$$\begin{aligned}
f_3(\mathbf{x}(k)) = {} & c_2(\mu(k+1))(\mu(k+2)-\mu(k+1))x_1(k+1)+x_5(k+1)+ \\
& c_1(\mu(k+1))c_4(\mu(k+1))(\mu(k+2)-\mu(k+1))x_3(k+1)+ \\
& ((m_{vr}v(k)r(k)+m_{wq}w(k)q(k)+d_u(k))/m_{11}+ \\
& u(k))\sin x_7(k+1)/(\cos\alpha(k+1)\cos\beta(k+1))
\end{aligned}$$

$$\begin{aligned}
f_4(\mathbf{x}(k)) = {} & \alpha_e(k+2)-\alpha_e(k+1)-c_2(\mu(k+1))(\mu(k+2)-\mu(k+1))+ \\
& d_q(k)/m_{44}+Tq(k)+\alpha(k+2)-\alpha(k+1)- \\
& c_2(\mu(k+1))(\mu(k+2)-\mu(k+1))
\end{aligned}$$

$$\begin{aligned}
f_5(\mathbf{x}(k)) = {} & \beta(k+2)-\beta(k+1)-c_1(\mu(k+1))(\mu(k+2)-\mu(k+1))+ \\
& (d_r(k)/m_{55}+Tr(k))/\cos\theta(k)+\beta(k+2)- \\
& \beta(k+1)-c_1(\mu(k+1))(\mu(k+2)-\mu(k+1))
\end{aligned}$$